

# Mechanical analysis of cutout piezoelectric nonlocal nanobeam including surface energy effects

Mohamed A. Eltahaer<sup>\*1,2</sup>, Fatema-Alzahraa Omar<sup>2</sup>, Waleed S. Abdalla<sup>2</sup>, Abdallah M. Kabeel<sup>2</sup>  
and Amal E. Alshorbagy<sup>2</sup>

<sup>1</sup>Mechanical Engineering Dept., Faculty of Engineering, King Abdulaziz University, Jeddah 21589, Saudi Arabia

<sup>2</sup>Mechanical Design and Production Dept., Faculty of Engineering, Zagazig University, Zagazig, 44519, Egypt

(Received February 21, 2018, Revised January 6, 2020, Accepted May 29, 2020)

**Abstract.** This manuscript tends to investigate influences of nanoscale and surface energy on a static bending and free vibration of piezoelectric perforated nanobeam structural element, for the first time. Nonlocal differential elasticity theory of Eringen is manipulated to depict the long-range atoms interactions, by imposing length scale parameter. Surface energy dominated in nanoscale structure, is included in the proposed model by using Gurtin–Murdoch model. The coupling effect between nonlocal elasticity and surface energy is included in the proposed model. Constitutive and governing equations of nonlocal-surface perforated Euler–Bernoulli nanobeam are derived by Hamilton’s principle. The distribution of electric potential for the piezoelectric nanobeam model is assumed to vary as a combination of a cosine and linear variation, which satisfies the Maxwell’s equation. The proposed model is solved numerically by using the finite-element method (FEM). The present model is validated by comparing the obtained results with previously published works. The detailed parametric study is presented to examine effects of the number of holes, perforation size, nonlocal parameter, surface energy, boundary conditions, and external electric voltage on the electro-mechanical behaviors of piezoelectric perforated nanobeams. It is found that the effect of surface stresses becomes more significant as the thickness decreases in the range of nanometers. The effect of number of holes becomes significant in the region  $0.2 \leq \alpha \leq 0.8$ . The current model can be used in design of perforated nano-electro-mechanical systems (PNEMS).

**Keywords:** perforated piezoelectric nanobeams; surface energy; nonlocal elasticity; mechanical behaviors; finite element method.

## 1. Introduction

Piezoelectric material that has coupling between mechanical and electrical properties, is known as smart material. This material is used broadly in many nano-applications, such as in nanogenerators (Wang and Song 2006), nanoresonators (Tanner *et al.* 2007) biosensors (Murmu and Adhikari 2012), micro/nanoelectromechanical systems (MEMS/NEMS) (Lazarus *et al.* 2012). These devices help the novel technological developments in many fields and cause industrial revolution. The exceedingly small sizes nanostructures (i.e. beams, sheets and plates) those are used as components in NEMS devices, present a significant challenge to researchers of nanomechanics, Eltahaer *et al.* (2019a).

The dimensions of nanostructures are very close to their interatomic distances. Thus, the size-effects are recognized to become more significant as the dimensions of structures reach to the nanoscale. The scale-independent concept of the classical continuum models causes some deficiencies and inaccurate results if they applied on those small-scale nanostructures. Micro-continuum field theories such as nonlocal theory, strain gradient theory, couple stress theory, Micromorphic theory, and surface energy are the extensions

of the classical field theories including micro/nanoscale space and time scales, Chen and Liew (2004). Nonlocal continuum theory has obtained much popularity among the researchers, because of its efficiency as well as simplicity to analyze the behavior of various nanostructures. This work is concerned with models developed according to the widely used nonlocal elasticity theory of Eringen and Edelen (1972), Eringen (1983), Eringen (1984). Otherwise, perforation is a very common process in (MEMS/NEMS) fabrication. Perforations can affect on the mechanical properties of sensors by both increasing the surface exposed and decreasing their volume (Rottenberg *et al.* 2013). Zand and Ahmadian (2009) investigated the vibrational behavior of electrostatically actuated microstructures subjected to nonlinear squeeze film damping and in-plane forces. Juntarasaid *et al.* (2012) developed the nonlocal elasticity to study bending and buckling of nanowires including the effects of surface stress by using the analytical and numerical solutions. Eltahaer *et al.* (2014) presented modified nonlocal functionally graded (FG) Timoshenko beam model to study static and buckling behaviors of nanobeams. Eltahaer *et al.* (2016) illustrated effects of thermal load and shear force on critical buckling and post-buckling loads of higher-order shear deformation nonlocal nanobeam.

Malikan (2018) investigated the buckling of a thick sandwich plate under the biaxial non-uniform compression using the modified couple stress theory. Zarei *et al.* (2018)

\*Corresponding author, Professor  
E-mail: [meltahaer@kau.edu.sa](mailto:meltahaer@kau.edu.sa); [mmeltahaer@zu.edu.eg](mailto:mmeltahaer@zu.edu.eg)

studied buckling and free vibration analysis of a circular tapered nanoplate subjected to in-plane forces. Eltahaer *et al.* (2018a&b) simulated the mechanical behaviors of the perforated nonlocal nanobeams. The formulation was based on the Euler–Bernoulli beam and Timoshenko beam with a nonlocal differential form of Eringen model. The effects of perforation size, number of cutouts and nonlocal parameter on the bending, buckling and vibration behaviors of perforated nanobeams were investigated. Eltahaer *et al.* (2018c) presented a modified continuum model to investigate the vibration behavior of CNTs by using both couple stress and energy equivalent models. Eltahaer *et al.* (2018d) analyzed crack of FG pipe under unsteady pressure and temperature in a natural gas facility by using finite element model. Faraji-Oskouie *et al.* (2019) derived the numerical solutions of original integral and differential formulations of Eringen's nonlocal model for static bending of Timoshenko beams. Hamed *et al.* (2019) presented effects of porosity models on static behavior of size dependent functionally graded beam. Eltahaer *et al.* (2019a) presented the influence of periodic (sine and cosine) and nonperiodic imperfections modes on buckling, postbuckling and dynamics of beam rested on nonlinear elastic foundations. Abdalrahmaan *et al.* (2019) and Almitani *et al.* (2019) presented a unified analytical model to investigate free and forced vibration responses of perforated thin and thick beams. Eltahaer *et al.* (2019b) exploited an energy equivalent model and finite element method to evaluate the equivalent Young's modulus of SWCNTs at any orientation angle by using tensile test. Mohamed *et al.* (2020) studied buckling and post-buckling behaviors of higher order carbon nanotubes using energy equivalent model. Eltahaer and Mohamed (2020) exploited doublet mechanics theory to investigate analytically nonlinear stability and vibration of imperfect CNTs.

Recently, the application of piezoelectric materials has been broadly spread in nano-structures including nonlocal elasticity and surface energy effects. Yan and Jiang (2011) used the Euler–Bernoulli beam theory to study the influence of surface effects, and surface piezoelectricity on the vibrational and buckling behaviors of piezoelectric nanobeams. Mahmoud *et al.* (2012) investigated static bending behavior of nanobeams including surface effects by nonlocal finite element. Sedighi (2014a) studied the influence of small scale on the pull-in behavior of nonlocal nanobridges considering surface effect, Casimir and Van der Waals attractions. Sedighi (2014b) presented the impact of vibrational amplitude on the dynamic pull-in instability and fundamental frequency of actuated microbeams Jandaghian (2016) analyzed analytically the problems of free vibration behavior of piezoelectric nanobeams with Eringen's nonlocal theory. Kheibari and Beni (2017) studied the free vibration of piezoelectric nanotubes by using Love's cylindrical thin-shell model. Effect of size, electromechanical, and geometric were investigated for the natural frequency of piezoelectric nanotubes including the Euler–Bernoulli and consistent couple stress theories.

Shishesaz *et al.* (2018) presented an analytical magneto-electro-mechanical model of a novel magneto-electro-elastic vibration-based energy harvesting system. Mahinzare *et al.* (2018) developed a formulation for the free

vibration analysis of functionally graded circular nanoplate in two directions. It had shown that the angular velocity, external electric voltage, size dependency and power-law index had significant effects on the natural frequency. Moory-Shirbani *et al.* (2018) analyzed experimentally and numerically a piezoelectrically actuated multilayered imperfect microbeam subjected to applied electric potential. Kerid *et al.* (2019) investigated the magnetic field, thermal loads and small-scale effects on the vibration of a perforated nanobeam structure based on Euler–Bernoulli beam model. Candelas *et al.* (2019) illustrated the Talbot effect using ultrasonic waves transmitted through a periodic perforated plate. Eltahaer *et al.* (2019c) demonstrated the coupling effects of nonlocal elasticity and surface properties on static and vibration characteristics of piezoelectric nanobeams with Euler–Bernoulli beam theory. Ansari *et al.* (2019) presented vibration analysis of functionally graded carbon nanotube-reinforced composite plates with cutout by using variational differential quadrature finite element method. Mohamed *et al.* (2019) studied mechanical behaviors of SWCNTs beam by using energy equivalent model. Ouakad and Sedighi (2019) studied static response and free vibration of MEMS arches assuming out-of-plane actuation pattern. Eltahaer and Mohamed (2020) derived the frequency equation of free vibration of nonlocal perforated nanobeams under general boundary conditions by using analytical method. Eltahaer *et al.* (2020) illustrated the effect of nonlocal elasticity on bending and vibration of nanobeams with geometrical cutouts. Bourouina *et al.* (2020) exploited non-local elasticity theory to present the influence of hole networks on the adsorption-induced frequency shift of a perforated nanobeam. Almitani *et al.* (2020) studied analytically the buckling behavior of perforated nanobeams incorporating surface energy effects.

The objective of the current work is to present a modified model capable of predicting the static bending and vibration behavior of perforated piezoelectric nanobeams including surface energy, which not be studied elsewhere. Analytical formulas for the equivalent geometrical characteristics of regularly squared perforated shape are developed. Kinematic assumption of thin Euler–Bernoulli thin beam theory is proposed. The size effect of nanostructure beam is considered by nonlocal Eringen elasticity and Gurtin–Murdoch surface theories. The manuscript is organized as follows: Section 2 presented geometrical adaptation for perforation, nonlocal and surface energy constitutive equations, and proposed mathematical detail. Section 3 contains numerical solution techniques by using finite element procedure. Section 4 presents numerical results and discusses influences of length-scale effect, surface parameters, perforation parameters, and electrical force on static and dynamic vibrations of piezoelectric nanobeam with cutouts. Finally, the main conclusions are summarized and listed in Section 5.

## 2. Mathematical formulation

### 2.1 Geometrical parameters

A piezoelectric nanobeam with regular square holes is illustrated in Fig. 1. As shown, the beam has length  $L$ , width  $b$ , and thickness  $h$ , with a pattern of regular square holes.

The spatial period between holes is  $l_s$  and with hole side  $l_s - t_s$ . The number of holes along the section is defined by  $N$ . So, the filling ratio of the beam can be depicted by (Abdelrahmaan *et al.* 2019 and Almitani *et al.* 2019)

$$\alpha = \frac{t_s}{l_s} \quad 0 \leq \alpha \leq 1 \quad (1)$$

As governing from previous equation, the beam is filled at filling ratio  $\alpha = 1$  and completely perforated at a filling ratio  $\alpha = 0$ . The normal stress will be abridged in the parts between holes, which will be under stressed with respect to the full beam case and will be over-stressed in the remaining parts. By assuming that the total stress along the cross section is the same for both complete beam and perforated one and assuming a linear continuous stress distribution in the filled segments, the equivalent bending stiffness can be defined (Luschi and Pieri 2014, Almitani *et al.* 2019, and Eltahir and Mohamed 2020)

$$(EI)_{eq} = EI \frac{\alpha(N+1)(N^2+2N+\alpha^2)}{(1-\alpha^2+\alpha^3)N^3+3\alpha N^2+(3+2\alpha-3\alpha^2+\alpha^3)\alpha^2 N+\alpha^3} \quad (2)$$

By integrating over the beam segment, the average mass of the perforated beam per unit length can be written as (Eltahir and Mohamed 2020, Bourouina *et al.* 2020)

$$(\rho A)_{eq} = \rho A * \frac{[1-N(\alpha-2)]\alpha}{N+\alpha} \quad (3)$$

## 2.2 Nonlocal perforated piezoelectric nanobeam including a surface effect

Based on the Euler–Bernoulli beam theory (EBT), the displacement filed of any point of the beam is given by Alshorbagy *et al.* (2011)

$$u(x, z, t) = u_0(x, t) - z \frac{\partial w_0(x, t)}{\partial x} \quad (4)$$

$$w(x, z, t) = w_0(x, t) \quad (5)$$

where  $t$  is the time and  $u_0(x, t)$  and  $w_0(x, t)$  are displacement components in the mid-plane along the  $x$  and  $z$ . The nonzero strain  $\varepsilon_{xx}$  of the Euler-Bernoulli beam theory is

$$\varepsilon_{xx} = \frac{\partial u_0}{\partial x} - z \frac{\partial^2 w_0(x, t)}{\partial x^2} = \varepsilon_{xx}^0 - z k^0 \quad (6)$$

Like the displacement field, the distribution of electric potential for the piezoelectric nanobeam model is assumed to vary as a combination of a cosine and linear variation, which satisfies the Maxwell's equation as (Jandaghian and Rahmani 2016),

$$\phi_{(x,z,t)} = -\cos(\beta z)\varphi(x, t) + \frac{2V}{h}z \quad (7)$$

The non-zero components of electric field  $E_x, E_z$  can be obtained as:

$$E_x = -\frac{\partial \varphi}{\partial x} = \cos(\beta z)\frac{\partial \varphi}{\partial x} \quad (8)$$

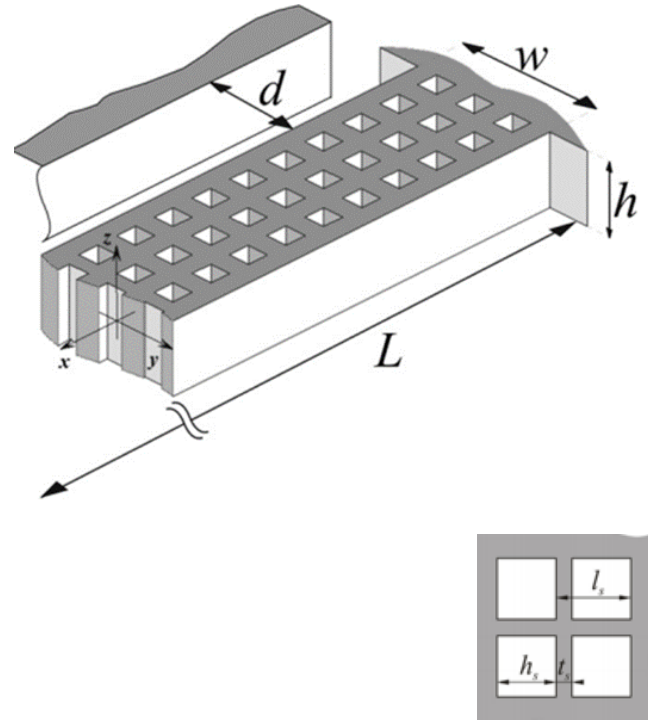


Fig. 1 Geometry of a perforated piezoelectric nanobeam with coordinate system (Luschi and Pieri 2016)

$$E_z = -\frac{\partial \varphi}{\partial z} = -\sin(\beta z)\varphi - \frac{2V}{h} \quad (9)$$

in which  $\beta = \pi/h$ ,  $\varphi(x, t)$  is the electric potential function in the  $x$ -direction that must satisfy the electric boundary conditions,  $z$  is measured from the mid-plane of the nanobeam in the transverse direction,  $h$  is the thickness of the piezoelectric nanobeam,  $V$  is the external electric voltage. The constitutive relation of the one-dimensional piezoelectric beam can be written as

$$\sigma_x = C_{11}\varepsilon_x - e_{31}E_z \quad (10)$$

$$D_z = e_{33}\varepsilon_x + K_{33}E_z \quad (11)$$

where  $\sigma_x$  is axial stress,  $D_z$  is electric displacement, and  $C_{11}$ ,  $e_{31}$  and  $K_{33}$  are elastic, piezoelectric and dielectric constants for the bulk medium.

In relation to the atomic features of nanostructures, there are always interactions between the elastic surface and the bulk material. To take the surface stress effects into account, Gurtin and Murdoch model is proposed, Ansari *et al.* (2015). As nanostructures submit in-plane loads in various directions, the stresses are created on the surfaces of the bulk of nanobeams. The constitutive relations of the surface layer can be expressed as

$$\sigma_{\alpha\beta}^s = \tau_s \delta_{\alpha\beta} + (\tau_s + \lambda_s)\varepsilon_{\gamma\gamma}\delta_{\alpha\beta} + 2(\mu_s - \tau_s)\varepsilon_{\alpha\beta} + \tau_s u_{\alpha\beta}^s, \quad (\alpha, \beta = x, y) \quad \& \quad (12)$$

$$\sigma_{\alpha z}^s = \tau_s u_{z,\alpha}^s$$

Therefore, the surface stress components can be derived with respect to the displacement constituents and can be written as

$$\sigma_{xx}^s = \tau_s + (\lambda_s + 2\mu_s) \frac{\partial u}{\partial x}, \quad \sigma_{xz}^s = \tau_s \frac{\partial w}{\partial x} \quad (13)$$

where  $\lambda_s$  and  $\mu_s$  as Lamé's surface constants and the surface residual tension  $\tau_s$ . According to the surface elasticity model, the constitutive equations for the surface layer of the piezoelectric nanobeam (PNB) can be obtained as, Huang and Yu (2006):

$$\sigma_x^s = \sigma_x^0 + C_{11}^s \epsilon_x - e_{31}^s E_z \quad (14)$$

$$D_x^s = D_x^0 \quad (15)$$

where  $\sigma_x^s$  and  $D_x^s$  are axial surface stress and surface electric displacement;  $\sigma_x^0$  and  $D_x^0$  are residual surface stress and residual surface electric displacement without applied strain and electric field; and  $C_{11}^s$  and  $e_{31}^s$  are surface elastic and surface piezoelectric constants. In the absence of free electric charges using Gauss's law:

$$\frac{\partial D_z}{\partial x} = 0 \quad (16)$$

Substituting Eq. (11) into Eq. (16) and using Eq. (6) and (9), and considering  $\varphi(-h/2) = 0$  and  $\varphi(h/2) = V$  as the electrical boundary conditions, the electric potential is expressed as, Eltahir et al. (2019c):

$$\varphi_{(x,z)} = -\frac{e_{31}}{2k_{33}} \frac{\partial^2 w(x,t)}{\partial x^2} \left( z^2 - \frac{h^2}{4} \right) + V \left( \frac{z}{h} + \frac{1}{2} \right) \quad (17)$$

The axial stresses for the bulk and the surface in Eq. (10) and (11) can be written as

$$\sigma_x = c_{11} \epsilon_0 - z \left( c_{11} + \frac{e_{31}^2}{k_{33}} \right) \frac{\partial^2 w(x,t)}{\partial x^2} + e_{31} \frac{V}{h} \quad (18)$$

$$\sigma_x^s = \sigma_x^0 + c_{11}^s \epsilon_0 - z \left( c_{11}^s + \frac{e_{31}^s e_{31}}{k_{33}} \right) \frac{\partial^2 w(x,t)}{\partial x^2} + e_{31}^s \frac{V}{h} \quad (19)$$

To impose the size effect of nanostructure, nonlocal piezoelectricity theory is proposed. This theory assumed that the stress tensor and the electric displacement at a reference point depend not only on the strain components and electric-field components at same position but also on all other points of the body Eltahir et al. (2019c), the nonlocal constitutive relation can be written as

$$\sigma_{ij} - (e_0 a)^2 \nabla^2 \sigma_{ij} = C_{ijkl} \epsilon_{kl} - e_{kij} E_K \quad (20)$$

$$D_i - (e_0 a)^2 \nabla^2 D_i = e_{ijkl} \epsilon_{kl} + \epsilon_{ij} E_K \quad (21)$$

where  $\sigma_{ij}$ ,  $\epsilon_{ij}$ ,  $D_i$  and  $E_i$  are the stress, strain, electric displacement and electric field, respectively;  $C_{ijkl}$ ,  $e_{kij}$ ,  $\epsilon_{ij}$  are the fourth-order elasticity tensor, piezoelectric constants, dielectric constants.

The governing equation for the piezoelectric beam considering surface effects can be written as, Liu & Rajapakse (2009) :

$$-\frac{\partial Q}{\partial x} + \int_S T_z ds - m_o \frac{\partial^2 w}{\partial t^2} = 0 \quad (22)$$

$$-\frac{\partial M}{\partial x} + Q + \int_S T_x z ds + N \frac{\partial w}{\partial x} = 0 \quad (23)$$

where Q is the shear force and S is the perimeter of the cross section, respectively. By differentiating Eq. (22) and substituting it into Eq. (23), we obtain the following Euler-Lagrange equation:

$$\frac{\partial^2 M}{\partial x^2} - \frac{\partial}{\partial x} \left( N \frac{\partial w}{\partial x} \right) + m_o \frac{\partial^2 w}{\partial t^2} - \frac{\partial}{\partial x} \int_S T_x z ds - \int_S T_z ds = 0 \quad (24)$$

in which, M is the bending moment and N is the axial normal force including the induced forces by the applied axial strain  $\epsilon_0$  and the applied electrical load,  $N = \int_A \sigma_x dA$ ,  $M = - \int_A \sigma_x z dA$ , the translated mass inertia of perforated beam is  $m_o = \int_A \rho dA = (\rho A)_{eq}$ .

The constitutive equation based on the nonlocal Euler-Bernoulli theory reads

$$M_{(x,t)} - \mu \frac{\partial^2 M_{(x,t)}}{\partial x^2} = -(EI)_{eff} \frac{\partial^2 w_{(x,t)}}{\partial x^2} \quad (25)$$

Direct substitution of Eq. (24) into Eq. (25), leads to the final expression for the non-local bending moment:

$$M_{(x,t)} = -(EI)_{eff} \frac{\partial^2 w_{(x,t)}}{\partial x^2} + \mu \left[ (\rho A)_{eq} \frac{\partial^2 w}{\partial t^2} - \frac{d}{dx} \left( (N)_{eff} \frac{\partial w_{(x,t)}}{\partial x} \right) \right] \quad (26)$$

using Eq. (26) and Eq. (24), leads to the nonlocal equation of motion for perforated piezoelectric nanobeams with surface effect:

$$(EI)_{eff} \frac{\partial^4 w_{(x,t)}}{\partial x^4} + \left[ 1 - \mu \frac{\partial^2}{\partial x^2} \right] \left[ (\rho A)_{eq} \frac{\partial^2 w_{(x,t)}}{\partial t^2} - \frac{d}{dx} \left( (N)_{eff} \frac{\partial w_{(x,t)}}{\partial x} \right) \right] = 0 \quad (27)$$

where  $(EI)_{eff}$  and  $(N)_{eff}$  are the effective bending rigidity and the effective axial load of the perforated piezoelectric nanobeam.  $A_t$ ,  $A_t^s$  are the area of the bulk and surface of the cross section.  $I_{tot}$ ,  $I_{tot}^s$  are the moment of inertia expressed as

$$(EI)_{eff} = \left\{ \left[ I_{tot} \left( C_{11} + \frac{e_{31}^2}{k_{33}} \right) + \left( \frac{e_{31}^s e_{31}}{k_{33}} + C_{11}^s \right) I_{tot}^s \right] \right. \\ \left. * \frac{\alpha(N+1)(N^2+2N+\alpha^2)}{(1-\alpha^2+\alpha^3)N^3+3\alpha N^2+(3+2\alpha-3\alpha^2+\alpha^3)\alpha^2 N+\alpha^3} \right\} \quad (28)$$

$$(N)_{eff} = A_t \varepsilon_0 c_{11} + (A_t^s/2) V e_{31} + A_t^s (\sigma_x^0 + C_{11}^s \varepsilon_0 + e_{31}^s \frac{V}{h}) \quad (29)$$

$$A_t = (W \cdot h) - N(hs \cdot h) \quad , \quad A_t^s = 2W - N(2h) \quad (30)$$

$$I_{tot} = \frac{W \cdot h^3}{12} - N \left( \frac{hs \cdot h^3}{12} \right) \quad , \quad I_{tot}^s = \left( \frac{W \cdot h^2}{2} + \frac{h^3}{6} \right) - N \left( \frac{hs \cdot h^2}{2} + \frac{h^3}{6} \right) \quad (31)$$

### 3. Numerical Formulation

Numerical solution procedure by using finite element method, is developed through this section to solve the mathematical model of perforated nonlocal nanobeam including a surface effect. The conventional Galerkin technique is employed to derive the weighted residual variation functional of the equilibrium. Denoting Galerkin's weight function by  $X$ , the variational formulation can be deduced by Eltahir *et al.* (2013) as

$$\int_0^T \sum_{e=1}^{ne} \left( \int_0^L (EI)_{eff} \frac{\partial^2 w_0}{\partial x^2} \frac{\partial^2 X}{\partial x^2} + \left[ (\rho A)_{eq} \frac{\partial w_0}{\partial t} \frac{\partial X}{\partial t} - (N)_{eff} \frac{\partial w_0}{\partial x} \frac{\partial X}{\partial x} \right] - \mu (\rho A)_{eq} \frac{\partial^2 w_0}{\partial x \partial t} \frac{\partial^2 X}{\partial x \partial t} + \mu (N)_{eff} \frac{\partial^2 w_0}{\partial x^2} \frac{\partial^2 X}{\partial x^2} \right) dx dt + \int_0^t \left[ \bar{N} \delta u_0 + \bar{V} \delta w_0 + \bar{M} \frac{\partial \delta w_0}{\partial x} \right]_0^L dt = 0 \quad (32)$$

The displacement field along the beam element in a local coordinate system, is described in terms of the Hermite interpolation functions as

$$\bar{w}(\bar{x}) = \sum_{i=1}^4 N_i U_i \quad (33)$$

where  $U_i$  denotes the nodal degrees of freedom, representing the deflection and rotation at each terminal node of the element; and  $N_i$ ,  $i = 1, 2, 3, 4$ , are the Hermite interpolation functions. By substituting Eq. (33) into the

Table 1 Material properties of PZT-5H

Bulk Properties			Surface Properties		
$c_{11}$	$\rho$	$e_{31}$	$\kappa_{33}$	$cs_{11}$	$es_{31}$
GPa	kg m <sup>-3</sup>	C m <sup>-2</sup>	C V <sup>-1</sup> m <sup>-1</sup>	N m <sup>-1</sup>	C m <sup>-1</sup>
126	7.5 × 10 <sup>3</sup>	-6.5	1.3 × 10 <sup>-8</sup>	7.56	-3 × 10 <sup>-8</sup>

Table 2 Maximum non-dimensional deflection of S-S beams

L/h	$\mu$	Analytical Reddy (2007)	Numerical Present results
20	0	1.313	1.3020
	1	1.4487	1.4270
	2	1.5844	1.5520
	3	1.7201	1.6770
	4	1.8558	1.8020
	5	1.9914	1.9270

modified weak form, Eq. (32), and performing the integration, we get the following equilibrium equation:

$$[[M_l] + [M_{nl}]]\{\ddot{\bar{W}}\} + [[K_l] + [K_b]]\{\bar{W}\} = 0 \quad (34)$$

where  $M$  and  $K$  are the element mass and stiffness matrices, respectively. The subscripts  $l, nl$ , and  $b$  donate the local, nonlocal, and buckling.

### 4. Numerical results

The static bending and free vibration of perforated piezoelectric nanobeams including a surface effect will be presented and discussed through this section. Influences of number of rows of holes, filling ratio, surface properties, nonlocal parameter, and external electric voltage on both static bending and natural frequency are presented and discussed. Assuming that the nanobeam is made of one kind of lead zirconate titanate material, PZT-5H with the bulk and surface material properties listed in Table.1, Yan and Jiang (2011). The length to thickness ratio of the nanobeam is fixed at  $L/h = 20$ , no initial axial strain exists (i.e,  $\varepsilon_0 = 0$ ), the beam thickness  $h=25$  nm and the beam width  $b=h$ . The following parameters are used in computing the numerical values:

#### 4.1 Static Analysis

To validate the proposed model, the deflection of simply supported (S-S) nonlocal nanobeam without any holes under uniform load and nonlocal parameter effect is compared with previously published results of Reddy (2007), as presented in Table 2. The nondimensional deflection is evaluated by  $\bar{w}_{max} = 100 * \delta_{max} * \frac{EI}{q_0 L^4}$ . As shown, the obtained results for maximum deflection are very close with Reddy's results.

The surface effects on the static deflection of piezoelectric nanobeam irrespective of the nonlocality and the electrical loads, where the beam thicknesses ( $h=25$  nm)

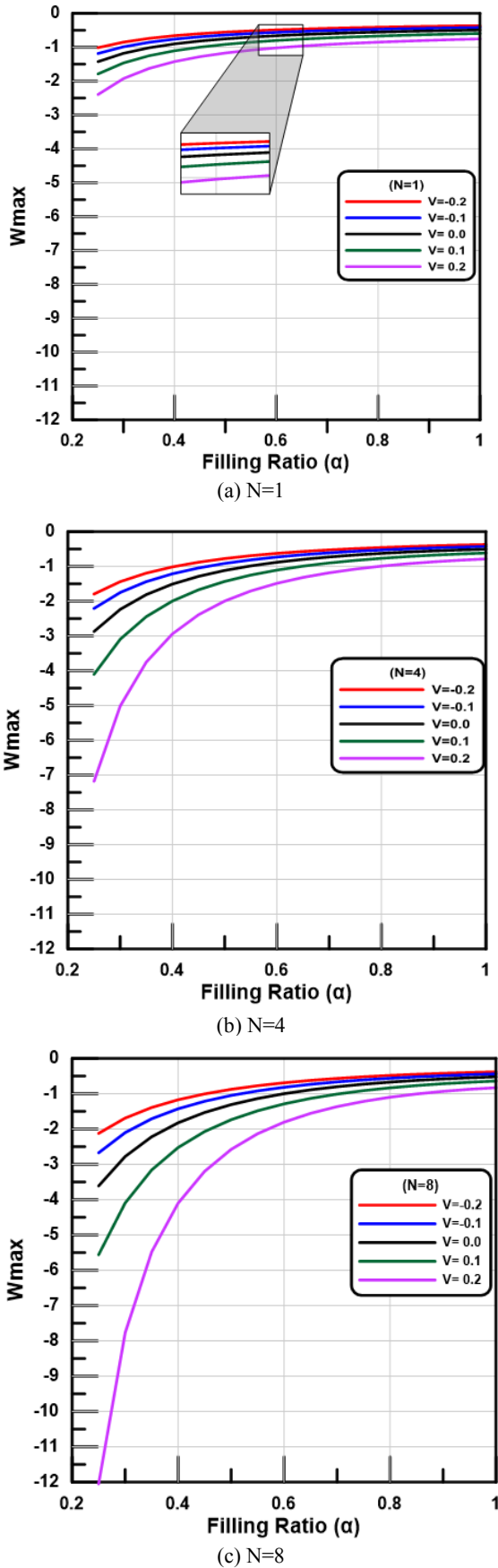


Fig. 2 Variation of normalized deflections against the filling ratio for perforated piezoelectric nanobeam at ( $\mu = 3 \times 10^{-14}$ ) under different electrical loads, V

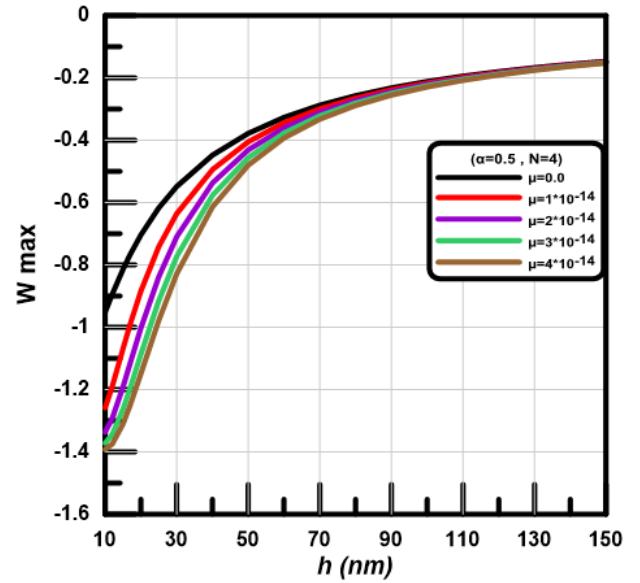


Fig. 3 Maximum central deflection against the beam thickness for different nonlocal parameter with applied voltage  $V = -0.1$  v

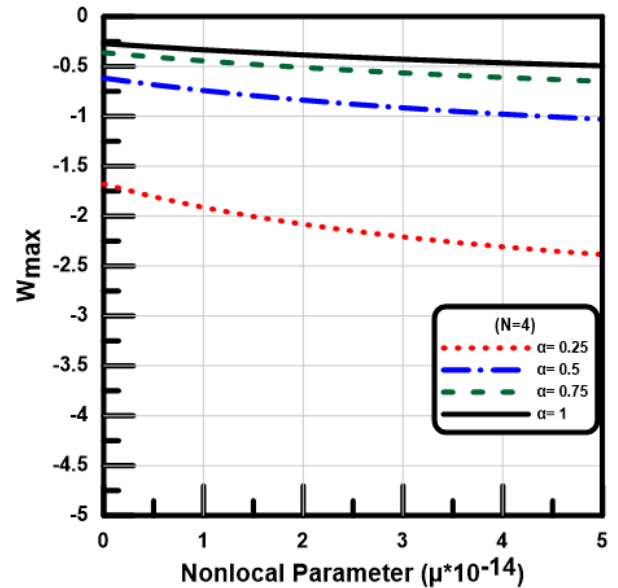


Fig. 4 Variation of normalized deflection against the nonlocal parameter for various filling ratios at ( $V = -0.1$ ,  $N = 4$ )

are investigated. Fig. 2 explains the variation of the normalized deflection with the filling ratios under different electrical loads ( $V$ ) at the number of holes along cross sectional ( $N = 1, 4, 8$ ) and the nonlocal parameter is ( $\mu = 3 \times 10^{-14}$ ). It's noted that, the maximum deflection increases by increasing the applied voltage for the perforated piezoelectric nanobeam. Also, the normalized deflection drops down with the increase of the filling ratio. The effects of number of holes become significant in the region  $0.2 \leq \alpha \leq 0.8$ . With the increase of the number of holes, the max deflection increases.

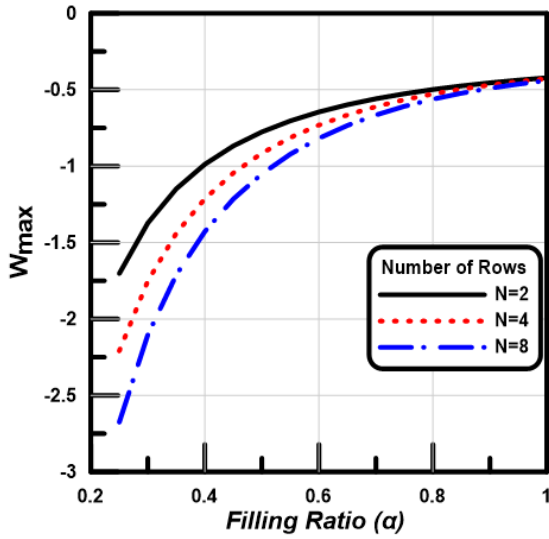


Fig. 5 Maximum central deflection against the filling ratios for different number of holes

Figure 3 illustrates the effect of the nonlocal parameter and surface effect on the non-dimensional deflection of the perforated piezoelectric nanobeam versus the thickness  $h$  with  $V = -0.1$ , filling ratio  $\alpha=0.5$  and number of holes  $N=4$ . It is observed that an increasing in the nonlocal parameter tends to increase the deflection, and by increasing the beam thickness  $h$ , the deflection will be reduced, due to increasing the rigidity of beam structure.

Figure 4 shows variation of the beam deflection with the nonlocal parameter for different values of the filling ratio at fixed value of the hole rows number  $N=4$ . Because of the beam softening resulting from increasing the nonlocal parameter, the max deflection increases with increasing the nonlocal parameter. Also, the deflection increases with decreasing the filling ratio due to the decrease of the bending stiffness.

The variation of the static bending with respect to the filling ratio for different number of hole rows at ( $v=-0.1$ ,  $\mu=3 \times 10^{-14}$ ) is presented in Fig. 5. It is observed that, for filling ratio greater than 0.8 the number of hole rows almost has no effect on the bending response of the perforated nanobeam. Also, it is noted, as the number of holes increased the maximum deflection increased. So that, the deflection is dependent on the coupling between the filling ratio and number of holes.

#### 4.2 Dynamic Analysis

Through this section, the model validation in dynamic analysis is presented and then followed by parametric studies to figure out effects of size-scale and perforation parameters on the fundamental frequencies of piezoelectric nanobeam with holes. The following equation should be solved to calculate fundamental frequencies:

$$[K][\bar{U}] = \omega^2 [M][\bar{U}] \quad (35)$$

In which  $\omega^2$  represents the fundamental frequency of perforated nanobeam, which has the nondimensional form

Table 3 Non-dimensional frequencies of the S-S beams for different nonlocal parameters.

L/h	$\mu$	Analytical	Numerical
		Reddy (2007)	Present results
20	0	9.8696	9.8797
	1	9.4159	9.4238
	2	9.0195	9.0257
	3	8.6693	8.6741
	4	8.3569	8.3606
	5	8.0761	8.0788

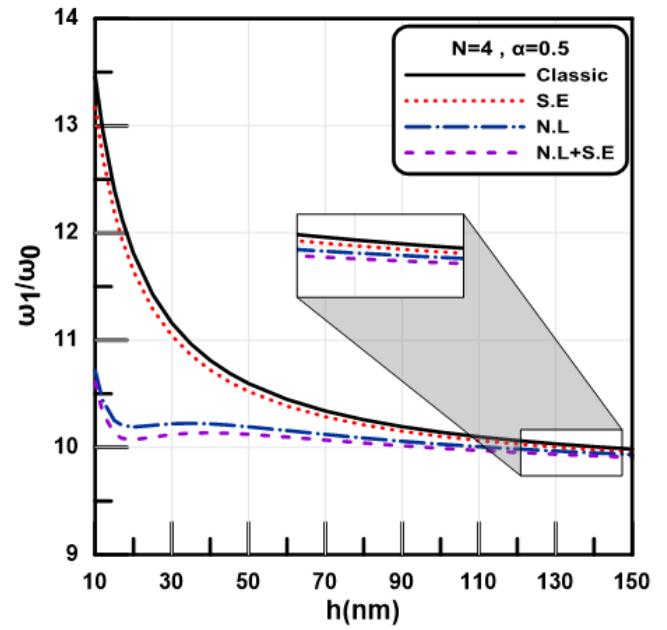


Fig. 6 Normalized frequency of the perforated piezoelectric nanobeams with various thicknesses for ( $V = 0$ ,  $\mu=1 \times 10^{-14}$ ).

$\lambda = \omega * L^2 * \sqrt{\rho A / EI}$ . The first flexural non-dimensional frequencies of the simply supported beam for different values of a nonlocal parameter are studied and compared with the results of Reddy (2007) as presented in Table 3. It is noted that the frequency of nanobeam is reduced by increasing the nonlocal parameter. This assures the significance of the nonlocal effect on the vibrational response of beams. According to Table 3, the present results are very close to Reddy's results. The validation of the full nanobeam including surface effect is present in previous work, Eltahir *et al.* (2019c).

Figure 6 illustrates the effect of the first nondimensional frequency for simply supported perforated piezoelectric nanobeam with different thicknesses at filling ratio  $\alpha=0.5$  and number of holes along cross-sectional is  $N=4$ . As shown in Fig.6 the effect of nanobeam thickness on normalized frequency for classical beam, surface effect (S.E), nonlocal effect (N.L) and the coupling effects of nonlocal theory and surface energy (S.E +N.L) of nanobeam. The effect of surface stresses becomes more significant as the thickness decreases in the range of

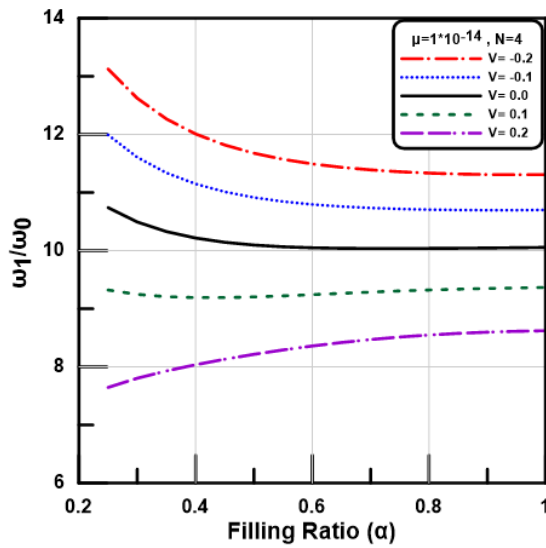


Fig. 7 Variation of the normalized frequency with the filling ratio for perforated piezoelectric nanobeam under different applied voltages, V

nanometers. In the nano regime, the nonlocality effect and the surface effects tend to decrease the fundamental frequency as the beam thickness increase. In both cases of surface and coupling effects, as the beam thickness increases from nanometer to micrometer and larger, the influence of the surface effects disappears, and the results converge to the classical natural frequencies model.

Figure 7 shows the variation of the 1<sup>st</sup> natural frequency for simply supported piezoelectric nanobeam against the filling ratio under different electrical loads (V) for ( $\mu = 1 \times 10^{-14}$ ,  $N = 4$ ). It's noted that, with the increase of the applied positive voltage, the normalized frequency decreases. In case of applied voltage ( $V=0.1, 0.2$ ), the natural frequencies increase, with the increase of the filling ratio. It is also observed, from this figure that the electromechanical coupling of piezoelectric materials can be explored for frequency tuning of nanobeams, as shown by the variation of the natural frequencies with the applied voltages.

Figure 8 shows the dependence of fundamental frequency on the coupling between filling ratio and number of holes along cross sectional of perforated piezoelectric nanobeams at a specified value of nonlocal parameter. It is noted that, the normalized frequencies decrease nonlinearly by increasing the filling ratio or increasing the number of holes along the cross-sectional. In case of ( $\mu=0.0$ ), the normalized frequency increases with filling ratio at any the value of N except 1. Also, the normalized frequency is decreased with increasing a filling ratio from 0.2 to 1 at ( $\mu \neq 0.0$ ). In case of ( $\mu=0.0$ ), the normalized frequency increases with filling ratio at any the value of N except 1. It is observed from Fig. 8 that, the effects of number of holes become insignificant in the region  $0.8 \leq \alpha \leq 1.0$ .

Figure 9 illustrates the effect of nonlocality on the fundamental frequency of perforated piezoelectric nanobeam at different boundary conditions BCs. The boundary conditions are (a) simply supported (S-S); (b) the

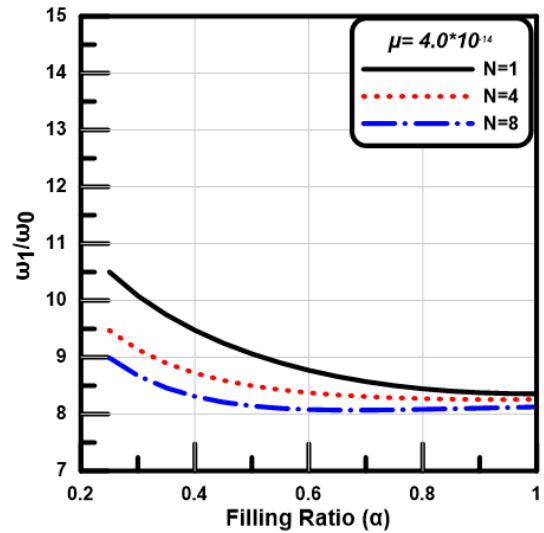
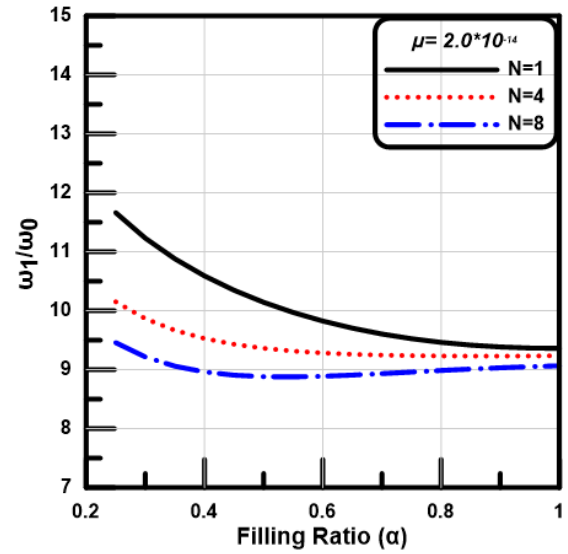


Fig. 8 the non-dimensional frequencies for different number of holes and various filling ratios at a specified value of nonlocal parameter

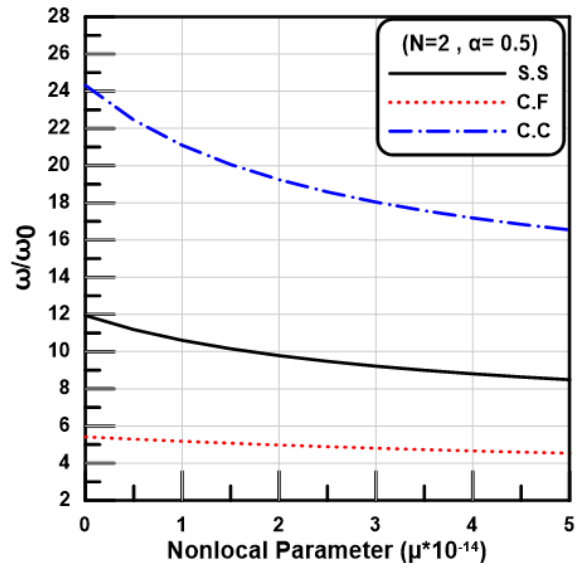


Fig. 9 The variation of the 1st frequency with nonlocal parameter at applied voltage ( $V=0.0$ )

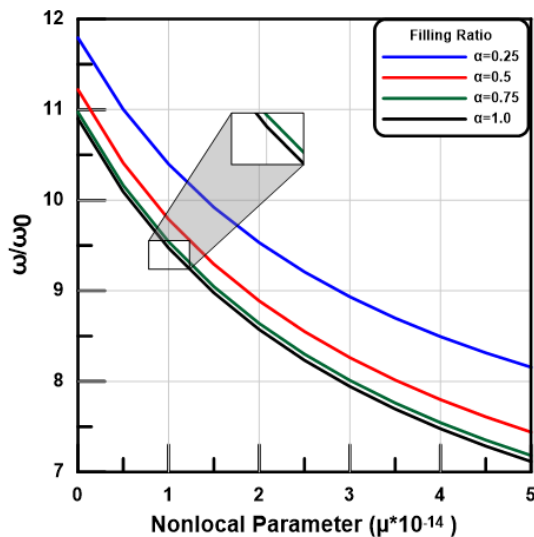


Fig. 10 The fundamental frequencies against the nonlocal parameter for various filling ratios

clamped- clamped (C–C); and (c) the cantilever (C–F) nanobeams. The normalized frequency is calculated for the beam taking into accounts the surface effects but with a zero applied voltage, the number of holes along cross-sectional  $N=2$  and the filling ratio  $\alpha=0.5$ . It can be concluded that, as the fundamental frequency decreases for all the cases of boundary conditions with the increase of nonlocal parameter.

The following results are obtained at fixed values of the hole rows number  $N=2$  and the electrical load  $V=0.1$ . Fig.10 shows variation of the fundamental frequencies against the nonlocal parameter for different values of the filling ratio, respectively. It can be concluded that the natural frequencies decrease with increasing the nonlocal parameter. The normalized frequency increases with decreasing the filling ratio.

## 5. Conclusions

This work is exploited to present a novel modified continuum model to study mechanical behaviors (static and vibration) of perforated piezoelectric nanobeams. The proposed model is based on Euler-Bernoulli hypothesis with a nonlocal differential form of Eringen model. Numerical results illustrate the effects of perforation parameters (perforation size and a number of cutouts), nonlocal parameter, external electric voltage, and boundary conditions on the bending and dynamic characteristics of the perforated nanobeam. The main conclusions derived from the results are:

*From static Analysis:* -

- The maximum deflection increases by increasing the applied voltage for the perforated piezoelectric nanobeam.
- The normalized deflection drops down with the increase of the filling ratio.
- The effects of number of holes become significant in the region  $0.2 \leq \alpha \leq 0.8$ . For filling ratio greater than 0.8,

the number of hole rows almost has no effect on the bending response of the perforated nanobeam.

- With the increasing of the number of holes, the max deflection will be increased.

*Form dynamic Analysis:* -

- The effect of surface stresses becomes more significant as the thickness decreases in the range of nanometers.
- In the nano regime, the nonlocality effect and the surface effects tend to decrease the fundamental frequency as the beam thickness increase.
- In both cases of surface and coupling effects, as the beam thickness increases from nanometer to micrometer and larger, the influence of the surface effects disappears, and the results converge to the classical natural frequencies model.
- The normalized frequency increases with decreasing the filling ratio.

## Acknowledgement

This work was supported by the Deanship of Scientific Research (DSR), King Abdulaziz University, Jeddah, under Grant no. (DF-523-135-1441). The authors, therefore, gratefully acknowledge the DSR technical and financial support.

## References

- Abdalrahmaan, A.A., Eltahir, M.A., Kabeel, A.M., Abdraboh, A.M., and Hendi, A.A. (2019). "Free and forced analysis of perforated beams", *Steel Compos. Struct.*, **31**(5), 489-502. <https://doi.org/10.12989/scs.2019.31.5.489>.
- Almitani, K.H., Abdalrahmaan, A.A., Eltahir, M.A., (2019), "On forced and free vibrations of cutout squared beams", *Steel Compos. Struct.*, **32**(5), 643-655. <https://doi.org/10.12989/scs.2019.32.5.643>.
- Almitani, K.H., Abdalrahmaan, A.A., Eltahir, M.A., (2020), "Stability of perforated nanobeams incorporating surface energy effects", *Steel Compos. Struct.*, **35**(4), 555-566. <https://doi.org/10.12989/scs.2020.35.4.555>.
- Alshorbagy, A. E., Eltahir, M. A. and Mahmoud, F. F. (2011), "Free vibration characteristics of a functionally graded beam by finite element method", *Appl. Math. Model.*, **35**(1), 412-425. <https://doi.org/10.1016/j.apm.2010.07.006>.
- Ansari, R., Gholami, R., Norouzzadeh, A. and Darabi, M. A. (2015), "Surface stress effect on the vibration and instability of nanoscale pipes conveying fluid based on a size-dependent Timoshenko beam model", *Acta Mechanica Sinica*, **31**(5), 708-719. <https://doi.org/10.1007/s10409-015-0435-4>.
- Ansari, R., Torabi, J. and Hassani, R. (2019), "Vibration analysis of FG-CNTRC plates with an arbitrarily shaped cutout based on the variational differential quadrature finite element method". *Mater. Res. Express*, **6**(12), 125086. <https://doi.org/10.1088/2053-1591/ab5b57>.
- Bourouina, H., Yahiaoui, R., Kerid, R., Ghoumid, K., Lajoie, I., Picaud, F. and Herlem, G. (2020), "The influence of hole networks on the adsorption-induced frequency shift of a perforated nanobeam using non-local elasticity theory", *J. Phys. Chem. Solids*, **136**, 109201. <https://doi.org/10.1016/j.jpcs.2019.109201>.

- Candelas, P., Fuster, J. M., Pérez-López, S., Uris, A. and Rubio, C. (2019), "Observation of ultrasonic Talbot effect in perforated plates", *Ultrasonics*, **94**, 281-284. <https://doi.org/10.1016/j.ultras.2018.08.019>.
- Chen, X. and Liew, K. (2004), "Buckling of rectangular functionally graded material plates subjected to nonlinearly distributed in-plane edge loads", *Smart Mater. Struct.*, **13**(6), 1430. <https://doi.org/10.1088/0964-1726/13/6/014>.
- Eltahaer, M., Alshorbagy, A. E. and Mahmoud, F. (2013), "Vibration analysis of Euler–Bernoulli nanobeams by using finite element method", *Appl. Math. Model.*, **37**(7), 4787-4797. <https://doi.org/10.1016/j.apm.2012.10.016>.
- Eltahaer, M. A., Mahmoud, F. F., Assie, A. E. and Meletis, E. I. (2013), "Coupling effects of nonlocal and surface energy on vibration analysis of nanobeams", *Appl. Math. Comput.*, **224**, 760-774. <https://doi.org/10.1016/j.amc.2013.09.002>.
- Eltahaer, M., Khairy, A., Sadoun, A. and Omar, F.-A. (2014), "Static and buckling analysis of functionally graded Timoshenko nanobeams", *Appl. Math. Comput.*, **229**, 283-295. <https://doi.org/10.1016/j.amc.2013.12.072>.
- Eltahaer, M. A., Khater, M. E., Park, S., Abdel-Rahman, E. and Yavuz, M. (2016), "On the static stability of nonlocal nanobeams using higher-order beam theories", *Adv. Nano Res.*, **4**(1), 51-64. <http://dx.doi.org/10.12989/anr.2016.4.1.051>.
- Eltahaer, M., Abdraboh, A. and Almitani, K. (2018a), "Resonance frequencies of size dependent perforated nonlocal nanobeam", *Microsyst. Technol.*, **24**, 3925-3937. <https://doi.org/10.1007/s00542-018-3910-6>.
- Eltahaer, M., Kabeel, A., Almitani, K. and Abdraboh, A. (2018b), "Static bending and buckling of perforated nonlocal size-dependent nanobeams", *Microsyst. Technol.*, **24**(12), 4881-4893. <https://doi.org/10.1007/s00542-018-3905-3>.
- Eltahaer, M. A., Agwa, M. and Kabeel, A. (2018c), "Vibration analysis of material size-dependent CNTs using energy equivalent model", *J. Appl. Comput. Mech.*, **4**(2), 75-86. <https://dx.doi.org/10.22055/jacm.2017.22579.1136>.
- Eltahaer, M. A., Attia, M. A., Soliman, A. E. and Alshorbagy, A. E. (2018d), "Analysis of crack occurs under unsteady pressure and temperature in a natural gas facility by applying FGM", *Struct. Eng. Mech.*, **66**(1), 97-111. <https://doi.org/10.12989/sem.2018.66.1.097>.
- Eltahaer, M. A., Mohamed, N., Mohamed, S. A. and Seddek, L. F. (2019a), "Periodic and nonperiodic modes of postbuckling and nonlinear vibration of beams attached to nonlinear foundations", *Appl. Math. Model.*, **75**, 414-445. <https://doi.org/10.1016/j.apm.2019.05.026>.
- Eltahaer, M. A., Almalki, T. A., Ahmed, K. I. and Almitani, K. H. (2019b), "Characterization and behaviors of single walled carbon nanotube by equivalent-continuum mechanics approach", *Adv. Nano Res.*, **7**(1), 39-49. <http://dx.doi.org/10.12989/anr.2019.7.1.039>.
- Eltahaer, M. A., Omar, F. A., Abdalla, W. S. and Gad, E. H. (2019c), "Bending and vibrational behaviors of piezoelectric nonlocal nanobeam including surface elasticity", *Wave Random Complex Media*, **29**(2), 264-280. <https://doi.org/10.1080/17455030.2018.1429693>.
- Eltahaer, M. A. and Mohamed, N. (2020), "Nonlinear Stability and Vibration of Imperfect CNTs by Doublet Mechanics", *Appl. Math. Comput.*, **382**, <https://doi.org/10.1016/j.amc.2020.125311>.
- Eltahaer, M.A., Mohamed, N.A., (2020), "Vibration of nonlocal perforated nanobeams under general boundary conditions", *Smart Struct. Syst.*, **25**(4), 501-514. <https://doi.org/10.12989/sss.2020.25.4.501>.
- Eltahaer, M.A., Omar F.A., Abdraboh, A.M., Abdalla, W.S., and Alshorbagy, A.E., (2020), "Mechanical behaviors of piezoelectric nonlocal nanobeam with cutouts", *Smart Struct. Syst.*, **25**(2), 219-228. <https://doi.org/10.12989/sss.2020.25.2.219>.
- Eringen, A. C. (1983), "On differential equations of nonlocal elasticity and solutions of screw dislocation and surface waves", *J. Appl. Phys.*, **54**(9), 4703-4710. <https://doi.org/10.1063/1.332803>.
- Eringen, A. C. (1984), "Plane waves in nonlocal micropolar elasticity", *J. Eng. Sci.*, **22**(8-10), 1113-1121. [https://doi.org/10.1016/0020-7225\(84\)90112-5](https://doi.org/10.1016/0020-7225(84)90112-5).
- Eringen, A. C. and Edelen, D. (1972), "On nonlocal elasticity", *J. Eng. Sci.*, **10**(3), 233-248. [https://doi.org/10.1016/0020-7225\(72\)90039-0](https://doi.org/10.1016/0020-7225(72)90039-0).
- Faraji-Oskouie, M., Norouzzadeh, A., Ansari, R. and Rouhi, H. (2019), "Bending of small-scale Timoshenko beams based on the integral/differential nonlocal-micropolar elasticity theory: a finite element approach", *Appl. Math. Mech.*, 1-16. <https://doi.org/10.1007/s10483-019-2491-9>.
- Gheshlaghi, B. and Hasheminejad, S. M. (2012), "Vibration analysis of piezoelectric nanowires with surface and small scale effects", *Current Appl. Phys.*, **12**(4), 1096-1099. <https://doi.org/10.1016/j.cap.2012.01.014>.
- Hamed, M. A., Sadoun, A. M. and Eltahaer, M. A. (2019), "Effects of porosity models on static behavior of size dependent functionally graded beam", *Struct. Eng. Mech.*, **71**(1), 89-98. <https://doi.org/10.12989/sem.2019.71.1.089>.
- Huang, G. Y. and Yu, S. W. (2006), "Effect of surface piezoelectricity on the electromechanical behaviour of a piezoelectric ring", *Physica Status Solidi (b)*, **243**(4), R22-R24. <https://doi.org/10.1002/pssb.200541521>.
- Jandaghian, A. and Rahmani, O. (2016), "An analytical solution for free vibration of piezoelectric nanobeams based on a nonlocal elasticity theory", *J. Mech.*, **32**(2), 143-151. <https://doi.org/10.1017/jmech.2015.53>.
- Jandaghian, A. A. and Rahmani, O. (2015), "On the buckling behavior of piezoelectric nanobeams: An exact solution", *J. Mech. Sci. Technol.*, **29**(8), 3175-3182. <https://doi.org/10.1007/s12206-015-0716-7>.
- Juntarasaid, C., Pulngern, T. and Chucheeepsakul, S. (2012), "Bending and buckling of nanowires including the effects of surface stress and nonlocal elasticity", *Physica E*, **46**, 68-76. <https://doi.org/10.1016/j.physe.2012.08.005>.
- Kerid, R., Bourouina, H., Yahiaoui, R., Bounekhla, M. and Aissat, A. (2019), "Magnetic field effect on nonlocal resonance frequencies of structure-based filter with periodic square holes network", *Physica E*, **105**, 83-89. <https://doi.org/10.1016/j.physe.2018.05.021>.
- Kheibari, F. and Beni, Y. T. (2017), "Size dependent electro-mechanical vibration of single-walled piezoelectric nanotubes using thin shell model", *Mater. Design*, **114**, 572-583. <https://doi.org/10.1016/j.matdes.2016.10.041>.
- Lazarus, A., Thomas, O. and Deü, J.-F. (2012), "Finite element reduced order models for nonlinear vibrations of piezoelectric layered beams with applications to NEMS", *Finite Elements Analysis Design*, **49**(1), 35-51. <https://doi.org/10.1016/j.finel.2011.08.019>.
- Liu, C. and Rajapakse, R. K. N. D. (2009), "Continuum models incorporating surface energy for static and dynamic response of nanoscale beams", *IEEE Transactions on Nanotechnology*, **9**(4), 422-431. <https://doi.org/10.1109/TNANO.2009.2034142>.
- Luschi, L. and Pieri, F. (2014), "An analytical model for the determination of resonance frequencies of perforated beams", *J. Micromechanics Microeng.*, **24**(5), 055004. <https://doi.org/10.1088/0960-1317/24/5/055004>.
- Luschi, L. and Pieri, F. (2016), "An analytical model for the resonance frequency of square perforated Lamé-mode resonators", *Sensors Actuators B Chem.*, **222**, 1233-1239. <https://doi.org/10.1016/j.snb.2015.07.085>.
- Mahinzare, M., Ranjbarpur, H. and Ghadiri, M. (2018), "Free vibration analysis of a rotary smart two directional functionally

- graded piezoelectric material in axial symmetry circular nanoplate”, *Mech. Syst. Signal Processing*, **100**, 188-207. <https://doi.org/10.1016/j.ymssp.2017.07.041>.
- Mahmoud, F. F., Eltahaer, M. A., Alshorbagy, A. E. and Meletis, E. I. (2012), “Static analysis of nanobeams including surface effects by nonlocal finite element”, *J. Mech. Sci. Technol.*, **26**(11), 3555-3563. <https://doi.org/10.1007/s12206-012-0871-z>.
- Malikan, M. (2018), “Buckling analysis of a micro composite plate with nano coating based on the modified couple stress theory”, *J. Appl. Comput. Mech.*, **4**(1), 1-15. <https://dx.doi.org/10.22055/jacm.2017.21820.1117>
- Mohamed, N., Eltahaer, M.A., Mohamed, S., and Seddek, L.F., (2019), “Energy Equivalent Model in Analysis of Postbuckling of Imperfect Carbon Nanotubes Resting on Nonlinear Elastic Foundation”, *Struct. Eng. Mech.*, **70**(6), 737-750. <https://doi.org/10.12989/sem.2019.70.6.737>.
- Mohamed, N., Mohamed, S. A. and Eltahaer, M. A. (2020), “Buckling and post-buckling behaviors of higher order carbon nanotubes using energy-equivalent model”, *Eng. Comput.*, 1-14. <https://doi.org/10.1007/s00366-020-00976-2>.
- Moory-Shirbani, M., Sedighi, H. M., Ouakad, H. M. and Najar, F. (2018), “Experimental and mathematical analysis of a piezoelectrically actuated multilayered imperfect microbeam subjected to applied electric potential”, *Compos. Struct.*, **184**, 950-960. <https://doi.org/10.1016/j.compstruct.2017.10.062>.
- Murmu, T. and Adhikari, S. (2012), “Nonlocal frequency analysis of nanoscale biosensors”, *Sensors Actuators A*, **173**(1), 41-48. <https://doi.org/10.1016/j.sna.2011.10.012>.
- Ouakad, H. M. and Sedighi, H. M. (2019), “Static response and free vibration of MEMS arches assuming out-of-plane actuation pattern”, *J. Non-Linear Mech.*, **110**, 44-57. <https://doi.org/10.1016/j.ijnonlinmec.2018.12.011>.
- Reddy, J. (2007), “Nonlocal theories for bending, buckling and vibration of beams”, *J. Eng. Sci.*, **45**(2-8), 288-307. <https://doi.org/10.1016/j.ijengsci.2007.04.004>.
- Rottenberg, X., Jansen, R., Cherman, V., Witvrouw, A., Tilmans, H., Zanaty, M., Khaled, A. and Abbas, M. (2013), “Meta-materials approach to sensitivity enhancement of MEMS BAW resonant sensors”, *Sensors*, Baltimore, MD, USA. 1-4. <https://doi.org/10.1109/ICSENS.2013.6688348>.
- Sedighi, H. M. (2014a), “The influence of small scale on the pull-in behavior of nonlocal nanobridges considering surface effect, Casimir and Van der Waals attractions”, *J. Appl. Mech.*, **6**(03), 1450030. <https://doi.org/10.1142/S1758825114500306>.
- Sedighi, H. M. (2014b), “Size-dependent dynamic pull-in instability of vibrating electrically actuated microbeams based on the strain gradient elasticity theory”, *Acta Astronautica*, **95**, 111-123. <https://doi.org/10.1016/j.actaastro.2013.10.020>.
- Shishesaz, M., Shirbani, M. M., Sedighi, H. M. and Hajnayeb, A. (2018), “Design and analytical modeling of magneto-electro-mechanical characteristics of a novel magneto-electro-elastic vibration-based energy harvesting system”, *J. Sound Vib.*, **425**, 149-169. <https://doi.org/10.1016/j.jsv.2018.03.030>.
- Tanner, S. M., Gray, J. M., Rogers, C., Bertness, K. A. and Sanford, N. A. (2007), “High-Q GaN nanowire resonators and oscillators”, *Appl. Phys. Lett.*, **91**(20), 203117. <https://doi.org/10.1063/1.2815747>.
- Wang, Z. L. and Song, J. (2006), “Piezoelectric nanogenerators based on zinc oxide nanowire arrays”, *Science*, **312**(5771), 242-246. <https://doi.org/10.1126/science.1124005>
- Yan, Z., and L. Y. Jiang. (2011), “The vibrational and buckling behaviors of piezoelectric nanobeams with surface effects”, *Nanotechnol.*, **22**(24), 245703. <https://doi.org/10.1088/0957-4484/22/24/245703>.
- Zand, M. M. and Ahmadian, M. (2009), “Vibrational analysis of electrostatically actuated microstructures considering nonlinear effects”, *Communications Nonlinear Sci. Numerical Simulation*, **14**(4), 1664-1678. <https://doi.org/10.1016/j.cnsns.2008.05.009>.
- Zarei, M., Faghani, G., Ghalami, M. and Rahimi, G. H. (2018), “Buckling and vibration analysis of tapered circular nano plate”, *J. Appl. Comput. Mech.*, **4**(1), 40-54. <https://dx.doi.org/10.22055/jacm.2017.22176.1127>.

CC